RSC Advances

PAPER

View Article Online
View Journal | View Issue

Cite this: *RSC Adv.*, 2015, **5**, 12872

In situ microfluidic fabrication of multi-shape inorganic/organic hybrid particles with controllable surface texture and porous internal structure†

Guannan Tang, Wenxiu Li, Xiaodong Cao and Hua Dong*

Received 30th September 2014
Accepted 5th January 2015

DOI: 10.1039/c4ra11492b

www.rsc.org/advances

In this study, multiple shapes like spherical, ellipsoidal, disk-like, and rod-like inorganic/organic hybrid particles are fabricated using droplet-based microfluidics. Instead of photo-polymerization, which is commonly used in previously reported studies, the diversity in particle configuration is realized *via* the fast hydrolysis of an organometallic compound. In comparison to inorganic/organic hybrid particles fabricated by directly incorporating inorganic components in the dispersed phase before droplet formation, our hybrid particles are synthesized *in situ* because the inorganic component is one of the hydrolysis products, which avoids the agglomeration or precipitation of inorganic components and thus ensures particle homogeneity. In this study, we demonstrate a new strategy by using hybrid particle containing poly (lactide-*co*-glycolide) (PLGA) and TiO_2 as a model material, among which TiO_2 is obtained from the hydrolysis of *n*-butyl titanate (TBT). The convoluted surface texture of PLGA/TiO_2 particles can be attributed to either the interfacial instabilities of droplets induced by *n*-butanol as the other hydrolysis product, or the elastic-driven wrinkling of the solid film generated on PLGA/TBT droplet surfaces through TBT hydrolysis. Moreover, due to the presence of hyper-dispersed *n*-butanol caused by localized TBT hydrolysis in the PLGA matrix, a porous internal structure can be formed in the PLGA/TiO_2 particle. We believe this strategy is versatile to fabricate numerous types of inorganic/organic hybrid particles, among which partial or all components can be synthesized through the quick hydrolysis of organometallic compounds.

Introduction

Particle fabrication *via* droplet-based microfluidics has become a world-wide research hotspot in recent years.[1–14] As an important subcategory of microfluidics, droplet-based microfluidics can generate and manipulate discrete droplets with precisely controlled volume and composition through shearing between immiscible phases in microchannels.[15] This technology shows several remarkable advantages, such as producing monodisperse particles with narrow size distribution, controlling the particle shape and structure in a multiple yet accurate manner, and generating droplets/particles of diverse materials such as inorganic compounds, gels, polymers or composites, among which the fabrication of nonspherical particles maybe the most attractive process. Owing to the anisotropic configuration, nonspherical particles exhibit unique hydrodynamic, electric, optical, catalytic, or magnetic properties and thus have significant applications in many fields.[16–19] However, most of the particles generated *via* traditional emulsion methods are spherical due to the minimization of interfacial free energy between the particle and the medium.[10] In contrast, multi-shape particles, such as spherical, disk-like, and rod-like, have been synthesized in droplet-based microfluidics,[20–27] which are often achieved *via* a photo-polymerization reaction in microchannels.[22–29] Although considerably advanced materials with various shapes have been successfully prepared, this strategy cannot be applied to all materials, especially those without photocurable components. Therefore, there is still an urgent need to explore new approaches to fabricate nonspherical particles in droplet-based microfluidics.

In addition to the particle shape, composition and porosity are also the fundamental properties of particulate materials. Compared with monocomponent particles, hybrid particles can combine the merits of individual components so as to meet the

National Engineering Research Center for Tissue Restoration and Reconstruction, Department of Biomedical Engineering, School of Materials Science and Engineering, South China University of Technology, Guangzhou, 510641, China. E-mail: donghua@scut.edu.cn

† Electronic supplementary information (ESI) available: SEM images of pure PLGA particles, pure TiO_2 particles and spherical PCL/TiO_2 particles, porous internal structure of PLGA/TiO_2 particles, TG-DSC data of pure PLGA and TiO_2 particles, morphology and size of TiO_2 in PLGA/TiO_2 particle, EDS analysis on the cross-section of PLGA/TiO_2 particle, contact angle measurement as a function of *n*-butanol concentration in the continuous phase. See DOI: 10.1039/c4ra11492b

complex requirements of practical applications. For hybrid particles containing inorganic and organic parts, their fabrication in droplet-based microfluidics are normally performed by directly incorporating inorganic particles (such as SiO_2, Fe_3O_4, and quantum dots) in the dispersed phase before droplet formation,[23,30–32] leading to the severe agglomeration or precipitation of inorganic components and thus poor homogeneity of hybrid particles. In addition, porosity control is another vital factor that should be considered in the particle fabrication process. Addition of porogens has been proven as an effective way to create porosity.[27,33] However, removal of porogens from the particles is time-consuming and the pores are not uniformly distributed from the inside.

In this study, we report a facile microfluidic strategy to fabricate spherical, ellipsoidal, disk-like, and rod-like inorganic/organic hybrid particles *via* hydrolysis of organometallic compounds. Specifically, herein, we demonstrate the synthesis of a model hybrid particle with TiO_2 as the inorganic component and poly (lactide-*co*-glycolide) (PLGA) as the organic component (in the following section, this hybrid material is labeled as PLGA/TiO_2 particle). The diversity in particle configuration is realized due to the fast hydrolysis of *n*-butyl titanate (TBT) dissolved in the dispersed phase and the as-formed stiff shell on the droplet surface. As a result, the PLGA/TiO_2 particles maintain the shape of liquid droplets in the microchannel. Moreover, it should be noted that the PLGA/TiO_2 particles are synthesized *in situ* because the inorganic component TiO_2 is one of the TBT hydrolysis products, which avoids the agglomeration or precipitation of inorganic components and ensures the particle homogeneity. Interestingly, the PLGA/TiO_2 particles display a convoluted surface texture and porous internal structure, possibly induced by the other hydrolysis product *n*-butanol or elastic-driven wrinkling. These particles show great potential in areas like drug delivery, biosensing, catalysis, coating, and tissue engineering.

Experimental section

Materials and reagents

PLGA (M_w = 30 kDa) with a 50 : 50 molar ratio of lactic to glycolic acid was purchased from Daigang Company (Zhengzhou, China). TBT and *n*-butanol were purchased from Fuchen Company (Tianjing, China). Glycerol and poly(vinyl alcohol) (PVA, M_w = 88 kDa) were purchased from Sinopharm and Aladdin Companies (China), respectively. Negative photoresist (NR21-20000P) was obtained from Futurrex (USA) and polydimethylsiloxane (PDMS, Sylgard 184) was purchased from Dow Corning (Midland, USA). All the materials and reagents were used as received without further purification.

Fabrication and surface treatment of microfluidic devices

Microfluidic flow-focusing devices were fabricated *via* standard soft lithography techniques. Firstly, a clean silicon wafer was spin-coated with negative photoresist. After baking at 80 °C for 10 min and 150 °C for 5 min, the resist was exposed to UV light through a photo-mask and developed in RD6 developer solution. The mixture of PDMS base and curing agent (10 : 1 w/w) was then poured onto the silicon wafer and cured at 60 °C to make a PDMS replica that was subsequently sealed with a glass slide *via* O_2 plasma. The width of branch channel and collection channel were 100 μm and 250 μm, respectively, and the depth of all channels was 100 μm. Surface treatment was conducted to improve the hydrophilicity of microchannels by injecting PVA/glycerol (2/5 wt%) aqueous solution and curing for 1 h.

Microfluidic fabrication of PLGA/TiO_2 hybrid particles

In our study, PLGA and TBT dissolved in dichloromethane were used as the dispersed phase, whereas an aqueous solution containing 90 wt% of glycerol and 0.5 wt% of PVA was used as the continuous phase. Both the dispersed phase and continuous phase were injected into the microfluidic devices using syringe pumps (Cole-Parmer, USA). Droplets could be produced continuously at the junction of the microchannels by controlling the flow rates of the dispersed phase and continuous phase. The as-prepared droplets were then collected in 2 wt% aqueous solution of PVA (if not otherwise specified), settled at room temperature for 24 h, centrifuged at a moderate speed, rinsed thoroughly by deionized water and finally dried in a freeze-drier (Lyophilizer, VIRTIS, USA).

Characterization of PLGA/TiO_2 hybrid particles

The morphology of PLGA/TiO_2 hybrid particles was observed using a field emission scanning electron microscope (FE-SEM, NOVA 430, Netherlands). The composition on the particle surface was examined with an electron probe micro-analyzer (EPMA, EPMA-1610, Shimadzu, Japan) and an attenuated total reflection Fourier transform infrared spectroscope (ATR-FTIR, Nexus Por Euro, USA). The valence state of Ti element was detected *via* an X-ray photoelectron spectrometer (XPS, Axis uHru DCD, England). The structure and content of TBT hydrolysis products in PLGA/TiO_2 hybrid particles was characterized by X-ray diffractometry (XRD, PANalytical, Netherlands), energy-dispersive X-ray spectroscopy (EDS, NOVA 430, Netherlands), as well as thermogravimetric and differential scanning calorimetry (TG-DSC, Diamond, Germany).

Results and discussion

Microfluidic flow-focusing devices were employed to generate monodisperse PLGA/TBT droplets, and these droplets were then solidified into PLGA/TiO_2 particles under the combined action of a chemical reaction (TBT hydrolysis) and a physical process (solvent extraction). Our primary results reveal that both spherical and nonspherical particles can be obtained. To figure out the inherent mechanism, we fabricated pure PLGA particles under the same conditions except for the removal of TBT from the dispersed phase. The as-prepared PLGA particles were all spherical (Fig. S1, ESI†) and independent of the flow rates of the dispersed phase and continuous phase, indicating the important role of TBT in the fabrication of nonspherical PLGA/TiO_2 particles. In our study, two types of situations may take place after the formation of the PLGA/TBT droplets: if TBT hydrolysis

is slower than solvent extraction, PLGA/TBT droplets would maintain liquid state at the outlet of the microfluidic device and become spherical in the collection solution, just like PLGA droplets; however, if TBT hydrolysis is much faster than solvent extraction, *i.e.*, TBT hydrolysis reaction occurs immediately after droplet formation, a solid shell might be produced on the droplet surface. As a result, the PLGA/TBT droplets can keep their shape in the collection channel even after flowing out of the device. It should be noted that the remaining TBT on the droplet surface would undergo more violent hydrolysis in the 2 wt% aqueous collection solution of PVA due to the higher concentration of water, and the particle configurations could be further enhanced. In order to verify our presumption, four types of PLGA/TBT droplets with spherical, ellipsoidal, disk-like and rod-like morphologies were deliberately generated in the microchannel by either controlling the flow rates of the dispersed and continuous phases or changing the size of the collection channel. As shown in Fig. 1, the resulting PLGA/TiO_2 particles show the same structure as the PLGA/TBT droplets, which is in good agreement with the second situation.

Unlike the traditional microfluidic fabrication of inorganic/organic hybrid particle, mixing inorganic components in the organic dispersed phase, PLGA/TiO_2 particles are synthesized *in situ* because TiO_2 is a product of TBT hydrolysis.[34,35] To confirm the success in hybrid particle preparation, the surface and bulk composition of PLGA/TiO_2 particles were first analyzed by EPMA, XPS, FTIR and TG-DSC with the results summarized in Fig. 2. Fig. 2a compares the EPMA profiles of PLGA, TiO_2 and PLGA/TiO_2 particles prepared in the same device. As can be seen, Ti element is absent from the surface of PLGA particle but present on the surface of TiO_2 and PLGA/TiO_2 particle, suggesting that Ti is originated from TBT hydrolysis. C and O elements observed on the surfaces of the three sample can be attributed to PLGA, which is the residual PVA surfactant or TBT hydrolysate. The valence state of Ti in hybrid particle was examined by XPS. The binding energies are 458.4 eV and 464.3 eV, corresponding to Ti $2p_{3/2}$ and Ti $2p_{1/2}$ of TiO_2, respectively (Fig. 2b). This proves that the TBT hydrolysis reaction is complete and the hydrolysates are TiO_2 and *n*-butanol.[36] To investigate the composition of solid shells on the hybrid particle surface, ATR-FTIR was performed and the data are shown in Fig. 2c. The broad and strong absorption peak at *ca.* 500–1000 cm^{-1} in curve d′ can be assigned to the Ti–O–Ti moiety of nanostructured TiO_2.[37] The absorption bands centered at 1394 and 1611 cm^{-1} can be attributed to the bending vibration of O–H,[38] indicating the presence of Ti–OH on the TiO_2 particle surface. The broad peak at 2600–3600 cm^{-1} is caused by H_2O; moreover, curve e′ shows the characteristic peaks of PLGA, including 1000–1450 cm^{-1} (C–H bending vibration), 1746 cm^{-1} (C=O stretching vibration) and 2800–3050 cm^{-1} (C–H stretching vibration). Evidently, peaks belonging to both PLGA and TiO_2 can be found in PLGA/TiO_2 hybrid particles (curve f′), and this observation proves that the solid film on the surface of PLGA/TiO_2 particle is composed of PLGA and TiO_2. The small shift of peaks in PLGA/TiO_2 particles, compared with those of pure PLGA and TiO_2, is possibly due to the interaction of PLGA and TiO_2 at the micro-/nano-scale.

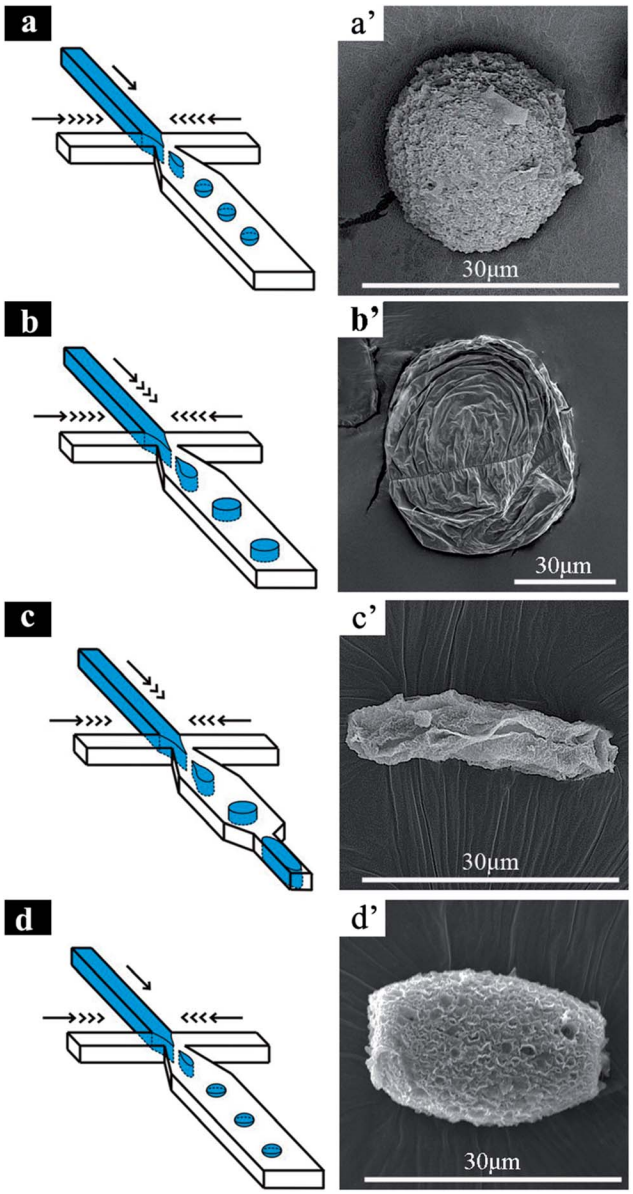

Fig. 1 Schematic illustration (a–d) and SEM images (a′–d′) of PLGA/TiO_2 particles with multiple shapes: (a and a′) spherical; (b and b′) disk-like; (c and c′) rod-like and (d and d′) ellipsoidal. Particle shape was determined by the relative ratio of the diameter *d* of the PLGA/TBT droplets to each dimension (*w*: width; *h*: height; $w > h$) of the collection channel: when $w > d$ and $h > d$ (a and a′), spherical particles were generated; when $w > d$ and $h < d$, disk-like particles were generated (b and b′); and when $w < d$ and $h < d$, rod-like particles were generated (c and c′). Ellipsoidal particles were obtained under a large flow rate of the continuous phase. The diameter *d* of PLGA/TBT droplets was adjusted by controlling the flow rates of the dispersed and continuous phases with the ratio indicated using arrows in the figure. Moreover, the width and height of the collection channel were changed by the mask of photolithography. Note that the microfluidic devices used in (a–c) were the same, *i.e.*, the width of branch channel and collection channel were 100 μm and 250 μm, respectively, and the depth of all channels was 100 μm. The microchannel in (d) was similar to that of (a–c) except that the collection channel was narrow near the outlet (the width was reduced from 250 μm to 100 μm).

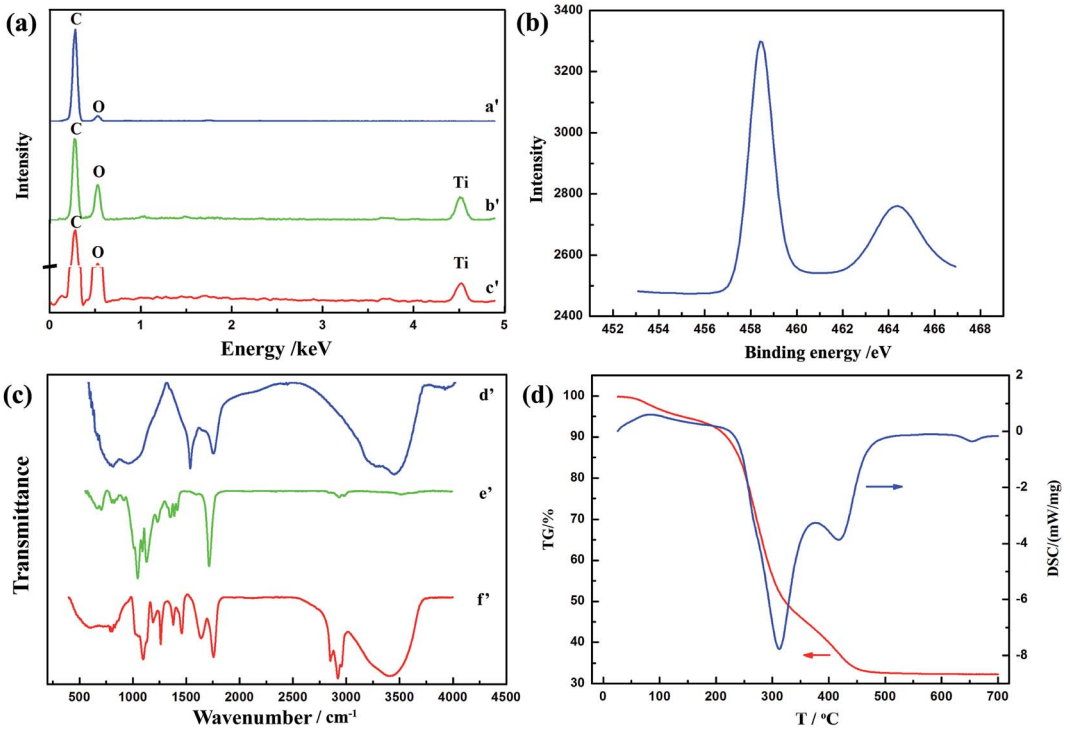

Fig. 2 Surface and bulk composition analysis and characterization of PLGA/TiO_2 particles: (a) EPMA profiles of (a′) PLGA, (b′) TiO_2, (c′) PLGA/TiO_2; (b) XPS data of PLGA/TiO_2 particles; (c) ATR-FTIR spectra of (d′) TiO_2, (e′) PLGA, (f′) PLGA/TiO_2; (d) TG-DSC curves for PLGA/TiO_2. All the samples were collected using the same microfluidic devices, except that the dispersed phases were pure PLGA, pure TBT and PLGA/TBT dissolved in dichloromethane. Note that the PLGA/TiO_2 particles used in (a and b) were prepared using a dispersed phase containing 8 mg g^{-1} TBT and 30 mg g^{-1} PLGA, whereas the PLGA/TiO_2 particles used in (c and d) were prepared using a dispersed phase containing 8 mg g^{-1} TBT and 7 mg g^{-1} PLGA.

Fig. 2d shows the TG-DSC curves of the PLGA/TiO_2 particle. The exothermic peaks at 311 °C and 417 °C refer to the combustion of PLGA and phase transition from anatase TiO_2 to rutile TiO_2 (see TG-DSC data of pure PLGA and TiO_2 in Fig. S2, ESI†).[36] In addition, the morphology and size of TiO_2 in PLGA/TiO_2 particle were further characterized *via* SEM after dissolving PLGA by acetone, and spherical TiO_2 with the size in the range of hundreds of nanometers to several micrometers can be observed (Fig. S3†). EDS analysis on the cross-section of PLGA/TiO_2 particle also reveals that TiO_2 is dispersed both on the particle surface and inside the particle (Table S1†).

In addition to the four basic particle shapes, another apparent feature of PLGA/TiO_2 particles is their convoluted surface texture. Considering the smooth surface of pure PLGA particles, the wrinkles on the hybrid particle surface can only result from TBT hydrolysis. To the best of our knowledge, the convoluted surface texture was once observed on polystyrene particles by Zhu *et al.*[10] and the reason was identified as the interfacial instabilities of emulsion droplet induced by *n*-hexadecanol. Since *n*-butanol can be *in situ* generated as a product of TBT hydrolysis, we can assume that interfacial instabilities of PLGA/TBT droplets are possible. According to the theory developed by Zhu and Hayward,[39] *n*-butanol, as a co-surfactant, can interpenetrate into the PVA monolayer at the organic/water interfaces and induces the rearrangement of PVA molecules. Hence, the interfacial tension can decrease dramatically or even vanish with the accumulation of *n*-butanol, driving interfacial roughening of the PLGA/TBT droplets. Our primary results of contact angle measurement also prove that the increase of *n*-butanol in the continuous phase can lead to a lower contact angle and thus lower interfacial tension on the PLGA/TiO_2 particle surface (Table S2, ESI†). As a result, the interfacial area will spontaneously increase by folding or deforming the interface. Another possible reason for surface roughing is elastic-driven wrinkling.[40] The solid film generated on PLGA/TBT droplet surface by fast hydrolysis of TBT may suffer buckling with the decrease in droplet volume and thus produce wrinkles on the particle surface. Nevertheless, after solvent extraction and TBT hydrolysis, the wrinkles on the droplet surface can be fixed.

The surface texture of PLGA/TiO_2 particles is not unchangeable but can be readily tailored by varying the PLGA and TBT concentrations in the dispersed phase. Take the disk-like particle for example, the increase in PLGA concentration leads to a less wrinkled particle surface, as presented in Fig. 3. The reason behind this can be understood either from the lower mass percentage of TBT and thus *n*-butanol in the droplet, which decreases the interfacial roughening speed or from the smaller volume change between liquid PLGA/TBT droplet and the solid PLGA/TiO_2 particle, which restricts the elastic-driven wrinkling effect. On the other hand, we also changed the TBT concentration, whereas kept the PLGA concentration constant.

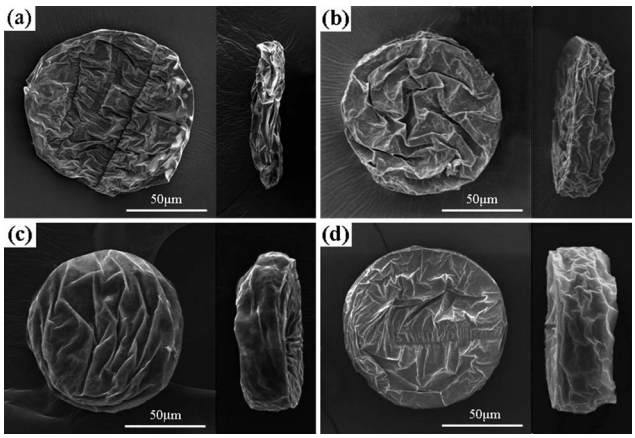

Fig. 3 SEM images of PLGA/TiO_2 particles fabricated with the dispersed phase containing constant TBT concentration (8 mg g^{-1}) and various PLGA concentrations: (a) 10 mg g^{-1}; (b) 30 mg g^{-1}; (c) 50 mg g^{-1}; (d) 70 mg g^{-1}. The continuous phase was aqueous solution containing 90 wt% of glycerol and 0.5 wt% of PVA, and the collection solution was 2 wt% aqueous solution of PVA. The thickness of PLGA/TiO_2 particles in (a–d) is 14.7, 23.5, 29.4 and 38.2 μm, respectively.

It can be seen from Fig. 4 that the surface roughness is enhanced when the concentration of TBT rises, and highly textured particles can be obtained when the TBT concentration is 12 mg g^{-1}. Although both the increase of PLGA concentration or decrease of TBT concentration may benefit the formation of smoother surface, more PLGA in dispersed phase indicates bigger particles, which reflects in our study as the thickening effects, whereas reduction of TBT does not change considerably with the particle size. This indicates that altering TBT concentration maybe a more effective way to control the surface texture of hybrid particles.

More interestingly, in comparison to the sliced PLGA particles, in which no pores can be observed (Fig. 5a), PLGA/TiO_2 particles display uniform porous internal structure without addition of porogens (Fig. 5b). The pore size falls in the range of 0.4–1.2 μm and appears invariable regardless of the PLGA concentration (Fig. S4 and S5, ESI†). To identify whether TiO_2 or *n*-butanol play the decisive role, another type of PLGA/TiO_2 particles were fabricated using the typical method reported in

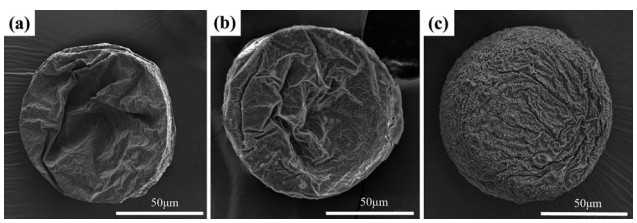

Fig. 4 SEM images of PLGA/TiO_2 particles fabricated with the dispersed phase containing a constant PLGA concentration (30 mg g^{-1}) and various TBT concentrations: (a) 4 mg g^{-1}; (b) 8 mg g^{-1}; (c) 12 mg g^{-1}. The continuous phase was aqueous solution containing 90 wt% of glycerol and 0.5 wt% of PVA, and the collection solution was 2 wt% aqueous solution of PVA. The particle thickness in (a–c) is similar (~22–25 μm).

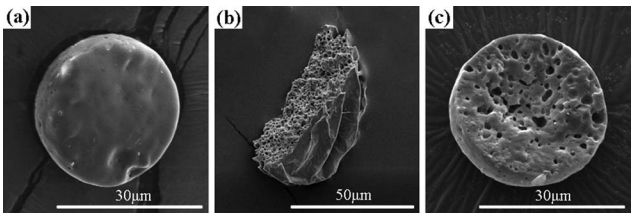

Fig. 5 Cross-section SEM images of sliced particles. These particles were fabricated using the dispersed phases containing (a) PLGA, (b) PLGA and TBT, (c) PLGA and *n*-butanol. The concentrations of PLGA, TBT and *n*-butanol were 70 mg g^{-1}, 8 mg g^{-1} and 7 mg g^{-1}, respectively. The concentration of *n*-butanol was calculated from that of TBT based on the hydrolysis reaction equation.

the previous studies, *i.e.*, mixing the nanosized TiO_2 in the dispersed phase. However, these PLGA/TiO_2 particles do not show the same porous structure as anticipated (data not shown here), indicative of little effect of TiO_2 on the formation of porous structure in PLGA/TiO_2 hybrid particle obtained by TBT hydrolysis. In contrast, PLGA particles prepared by directly adding *n*-butanol in the dispersed phase exhibit a porous internal structure, but the pores are much larger and unevenly distributed (Fig. 5c). Nevertheless, this observation confirms the possibility of *n*-butanol as a porogen. Although more experiments are still required before drawing a final conclusion, the well-distributed pores in PLGA/TiO_2 particles can be ascribed to the dense surface film and localized TBT hydrolysis (or namely, localized generation of *n*-butanol). As stated above, TBT hydrolysis is initially very fast on the droplet/water interface and then generates a solid surface film. Subsequently, the TBT hydrolysis is slowed down due to the compactness and hydrophobicity of surface film, which hinders the diffusion of water into the droplets. In such a case, solvent extraction rate might equal to or even exceed TBT hydrolysis rate, resulting in localized micro-phase separation between solid PLGA and liquid TBT. When water diffuses across the PLGA matrix to the tiny TBT droplets, hydrolysis reaction occurs and generates hyper-dispersed *n*-butanol. Once the PLGA/TiO_2 particles are freeze-dried, the hyper-dispersed *n*-butanol is volatilized and leaves a uniform pore structure. Fig. 6 shows the schematic illustration of this process. For those PLGA particles produced after addition of *n*-butanol, solvent extraction is accompanied with the

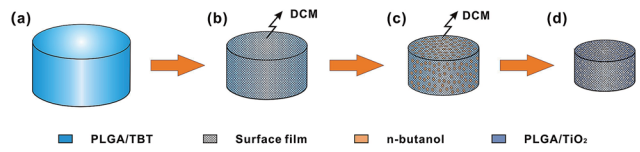

Fig. 6 Schematic illustration of the formation mechanism of the porous internal structure inside disk-like PLGA/TiO_2 particles. (a) PLGA/TBT droplets are first produced at the junction of microchannels; (b) TBT hydrolysis occurs on the droplet/water interface and a solid film is generated; (c) hyper-dispersed *n*-butanol results from the localized TBT hydrolysis in PLGA matrix; (d) a porous internal structure is formed *via* a freeze-drying process in which *n*-butanol is volatilized.

fusion of *n*-butanol into small droplets inside the particle, which could finally develop into big holes after freeze drying.

In our study, a series of PLGA/TiO_2 particles were fabricated with the TiO_2 content in the range of 0.1–21.2 wt%; moreover, it should be noted that high TiO_2 content can be achieved *via* the reduction of PLGA concentration (see disk-like TiO_2 particles without PLGA in Fig. S6, ESI†). Furthermore, it should be noted that the strategy developed herein is not limited to the fabrication of multi-shape PLGA/TiO_2 particles. Actually, we also replaced PLGA with poly (ε-caprolactone) (PCL) and prepared PCL/TiO_2 particles (Fig. S7, ESI†). In a broader perspective, this strategy is versatile to fabricate numerous types of particles, among which partial or all components can be synthesized through the quick hydrolysis of organometallic compounds.

Conclusion

In summary, we describe the *in situ* microfluidic synthesis of multi-shape PLGA/TiO_2 hybrid particles with a controllable surface texture and a porous internal structure. Because of the quick TBT hydrolysis, spherical, ellipsoidal, disk-like and rod-like PLGA/TiO_2 particles can be obtained by controlling the shape of PLGA/TBT droplets in the microchannel, which is achieved *via* the adjustment of flow rates of the dispersed and continuous phases as well as the size of the collection channel. The convolution of particle surface is possibly caused by either the interfacial instabilities of droplets induced by *n*-butanol as the other hydrolysis product or elastic-driven wrinkling of the solid film generated on PLGA/TBT droplet surface through TBT hydrolysis. Moreover, the surface roughness of the hybrid particle can be tuned readily by manipulating the relative concentration ratio between PLGA and TBT in the dispersed phase. Due to the presence of hyper-dispersed *n*-butanol, caused by localized TBT hydrolysis, porous internal structures can be generated in a PLGA/TiO_2 particle. We believe this strategy is suitable to fabricate numerous types of inorganic/organic hybrid particles, among which partial or all components can be synthesized through the quick hydrolysis of organometallic compounds.

Conflict interest

The authors declare no competing financial interest.

Acknowledgements

This research work was financially sponsored by the National Natural Science Foundation of China (Grant no. 21105029, 51373056, 51372085), the Program for New Century Excellent Talents in University (NCET-11-0150) and the Fundamental Research Funds for the Central Universities (2012ZZ0089).

References

1 A. S. Utada, E. Lorenceau, D. R. Link, P. D. Kaplan, H. A. Stone and D. A. Weitz, *Science*, 2005, **308**, 537.
2 C. Liang-Yin, A. S. Utada, R. K. Shah, K. Jin-Woong and D. A. Weitz, *Angew. Chem., Int. Ed.*, 2007, **46**, 8970.
3 K. Shin-Hyun and D. A. Weitz, *Angew. Chem., Int. Ed.*, 2011, **50**, 8731.
4 T. Nisisako, S. Okushima and T. Torii, *Soft Matter*, 2005, **1**, 23.
5 M. Seo, C. Paquet, Z. H. Nie, S. Q. Xu and E. Kumacheva, *Soft Matter*, 2007, **3**, 986.
6 J. Y. Wang, Y. D. Hu, R. H. Deng, W. J. Xu, S. Q. Liu, R. J. Liang, Z. H. Nie and J. T. Zhu, *Lab Chip*, 2012, **12**, 2795.
7 Y. H. Chen, G. Nurumbetov, R. Chen, N. Ballard and S. A. F. Bon, *Langmuir*, 2013, **29**, 12657.
8 Y. H. Wang, E. Tumarkin, D. Velasco, M. Abolhasani, W. Lau and E. Kumacheva, *Lab Chip*, 2013, **13**, 2547.
9 Y. Liu, M. H. Ju, C. Q. Wang, L. X. Zhang and X. Q. Liu, *J. Mater. Chem.*, 2011, **21**, 15049.
10 S. Q. Liu, R. H. Deng, W. K. Li and J. T. Zhu, *Adv. Funct. Mater.*, 2012, **22**, 1692.
11 S. Y. Teh, R. Khnouf, H. Fan and A. P. Lee, *Biomicrofluidics*, 2011, **5**, 44113.
12 Y. C. Pan, M. H. Ju, C. Q. Wang, L. X. Zhang and N. P. Xu, *Chem. Commun.*, 2010, **46**, 3732.
13 S. Ota, S. Yoshizawa and S. Takeuchi, *Angew. Chem., Int. Ed.*, 2009, **48**, 6533.
14 N. Prasad, J. Perumal, C. H. Choi, C. S. Lee and D. P. Kim, *Adv. Funct. Mater.*, 2009, **19**, 1656.
15 J. T. Wang, J. Wang and J. J. Han, *Small*, 2011, **7**, 1728.
16 C. Burda, X. B. Chen, R. Narayanan and M. A. El-Sayed, *Chem. Rev.*, 2005, **105**, 1025.
17 G. Hodes, *Adv. Mater.*, 2007, **19**, 639.
18 G. M. Whitesides, *Small*, 2005, **1**, 172.
19 Y. Xia, P. Yang, Y. Sun, Y. Wu, B. Mayers, B. Gates, Y. Yin, F. Kim and H. Yan, *Adv. Mater.*, 2003, **15**, 353.
20 S. Sugiura, T. Oda, Y. Izumida, Y. Aoyagi, M. Satake, A. Ochiai, N. Ohkohchi and M. Nakajima, *Biomaterials*, 2005, **26**, 3327.
21 W. H. Tan and S. Takeuchi, *Adv. Mater.*, 2007, **19**, 2696.
22 D. Dendukuri, K. Tsoi, T. A. Hatton and P. S. Doyle, *Langmuir*, 2005, **21**, 2113.
23 S. Q. Xu, Z. H. Nie, M. Seo, P. Lewis, E. Kumacheva, H. A. Stone, P. Garstecki, D. B. Weibel, I. Gitlin and G. M. Whitesides, *Angew. Chem., Int. Ed.*, 2005, **44**, 724.
24 Z. H. Nie, W. Li, M. Seo, S. Q. Xu and E. Kumacheva, *J. Am. Chem. Soc.*, 2006, **128**, 9408.
25 D. K. Hwang, D. Dendukuri and P. S. Doyle, *Lab Chip*, 2008, **8**, 1640.
26 R. F. Shepherd, J. C. Conrad, S. K. Rhodes, D. R. Link, M. Marquez, D. A. Weitz and J. A. Lewis, *Langmuir*, 2006, **22**, 8618.
27 A. Abbaspourrad, N. J. Carroll, S. H. Kim and D. A. Weitz, *Adv. Mater.*, 2013, **25**, 3215.
28 S. N. Yin, C. F. Wang, Z. Y. Yu, J. Wang, S. S. Liu and S. Chen, *Adv. Mater.*, 2011, **23**, 2915.
29 S. Seiffert, M. B. Romanowsky and D. A. Weitz, *Langmuir*, 2010, **26**, 14842.
30 Y. J. Jiang, J. H. Jiang, Q. M. Gao, M. L. Ruan, H. M. Yu and L. J. Qi, *Nanotechnology*, 2008, **19**, 075714.

31 S. I. Stoeva, F. W. Huo, J. S. Lee and C. A. Mirkin, *J. Am. Chem. Soc.*, 2005, **127**, 15362.
32 D. L. Shi, H. S. Cho, Y. Chen, H. Xu, H. C. Gu, J. Lian, W. Wang, G. K. Liu, C. Huth, L. M. Wang, R. C. Ewing, S. Budko, G. M. Pauletti and Z. Y. Dong, *Adv. Mater.*, 2009, **21**, 2170.
33 S. Dubinsky, H. Zhang, Z. H. Nie, I. Gourevich, D. Voicu, M. Deetz and E. Kumacheva, *Macromolecules*, 2008, **41**, 3555.
34 S. A. Khan and K. F. Jensen, *Adv. Mater.*, 2007, **19**, 2556.
35 M. Takagi, T. Maki, M. Miyahara and K. Mae, *Chem. Eng. J.*, 2004, **101**, 269.
36 J. H. Tian, P. F. Gao, Z. Y. Zhang, W. H. Luo and Z. Q. Shan, *Int. J. Hydrogen Energy*, 2008, **33**, 5686.
37 J. F. Ye, W. Liu, J. G. Cai, S. Chen, X. W. Zhao, H. H. Zhou and L. M. Qi, *J. Am. Chem. Soc.*, 2011, **133**, 933.
38 J. Das, F. S. Freitas, I. R. Evans, A. F. Nogueirab and D. Khushalani, *J. Mater. Chem.*, 2010, **20**, 4425.
39 J. T. Zhu and R. C. Hayward, *Angew. Chem., Int. Ed.*, 2008, **130**, 7496.
40 Y. Sugiyama, R. J. Larsen, J. W. Kim and D. A. Weitz, *Langmuir*, 2006, **22**, 6024.